JGR Biogeosciences

RESEARCH ARTICLE
10.1029/2021JG006441

Winter Daytime Warming and Shift in Summer Monsoon Increase Plant Cover and Net CO_2 Uptake in a Central Tibetan Alpine Steppe Ecosystem

Felix Nieberding[1,2], Christian Wille[2], Yaoming Ma[3,4,5], Yuyang Wang[3,4,5], Philipp Maurischat[6], Lukas Lehnert[7], and Torsten Sachs[2,8]

[1]Institute of Geosystems and Bioindication, Technische Universität Braunschweig, Braunschweig, Germany, [2]GFZ German Research Centre for Geosciences, Potsdam, Germany, [3]Key Laboratory of Tibetan Environment Changes and Land Surface Processes, Institute of Tibetan Plateau Research, Chinese Academy of Sciences, Beijing, China, [4]CAS Center for Excellence in Tibetan Plateau Earth Sciences, Beijing, China, [5]University of Chinese Academy of Sciences, Beijing, China, [6]Institute of Soil Science, Leibniz Universität Hannover, Hanover, Germany, [7]Department of Geography, Ludwig-Maximilians-Universiät München, Munich, Germany, [8]Institute of Flight Guidance, Technische Universität Braunschweig, Braunschweig, Germany

Abstract Over the past decades, human-induced climate change has led to a widespread wetting and warming of the Tibetan Plateau (TP), affecting both ecosystems and the carbon cycling therein. Whether the previously observed climate changes stimulate carbon uptake via enhanced photosynthesis or carbon loss via enhanced soil respiration remains unclear. Here we present 14 years of observations of carbon fluxes, meteorological variables and remotely sensed plant cover estimations from a central Tibetan alpine steppe ecosystem at Nam Co, the third largest lake on the TP. Using modified Mann-Kendall trend tests, we found a significant increasing daily net carbon uptake of 0.5 g C m^{-2} $decade^{-1}$, which can be explained by a widespread greening at the southern shore of lake Nam Co. The Plateau-wide changes in temperature and precipitation are locally expressed as an increasing diurnal temperature range during winter, higher water availability during spring, higher cloud cover during early summer and less water availability during late summer. While these changes differ over the course of the year, they tend to stimulate plant growth more than microbial respiration, leading to an increased carbon uptake during all seasons. This study indicates that during the 14 years study period, a higher amplitude in winter temperatures and an earlier summer monsoon promote carbon uptake in a central Tibetan alpine steppe ecosystem.

Plain Language Summary Similar to the northern and southern high latitudes, global warming is especially pronounced on the Tibetan Plateau (TP). It remains uncertain, in which way the alpine short grass steppe responds to the observed warming and wetting of the TP. By analyzing nearly 14 years of data describing the carbon dioxide (CO_2) exchange between the steppe and the atmosphere, we found that the ecosystem acts as a small carbon sink during recent years. Furthermore, we found that the steppe is becoming greener and stores more CO_2 during our study period. The trend in carbon uptake can be attributed to different mechanisms for different seasons. During winter, higher daytime temperatures promote plant growth which leads to higher uptake of CO_2 through photosynthesis. An earlier summer monsoon provides more cloud cover during early summer, which relieves drought stress from the plants, thus increasing photosynthetic uptake of CO_2. We observed increasing drought conditions during late summer, which hampers soil respiration stronger than plant growth. Together, these changes lead to stronger and earlier greening of the central Tibetan alpine steppe ecosystem and to more carbon storage than release.

Key Points:

- A widespread greening of the alpine steppe at Nam Co was observed, increasing the daily ecosystem carbon uptake by 0.5 g C m^{-2} decade-1
- Larger diurnal temperature range during winter promotes plant growth more than soil respiration
- Earlier summer monsoon cloud cover and greater aridity in autumn both lead to increased net carbon uptake during these times

Supporting Information:

Supporting Information may be found in the online version of this article.

Correspondence to:

F. Nieberding and Y. Ma,
felix.nieberding@posteo.de;
ymma@itpcas.ac.cn

Citation:

Nieberding, F., Wille, C., Ma, Y., Wang, Y., Maurischat, P., Lehnert, L., & Sachs, T. (2021). Winter daytime warming and shift in summer monsoon increase plant cover and net CO_2 uptake in a central Tibetan alpine steppe ecosystem. *Journal of Geophysical Research: Biogeosciences*, *126*, e2021JG006441. https://doi.org/10.1029/2021JG006441

Received 11 MAY 2021
Accepted 20 SEP 2021

Author Contributions:

Conceptualization: Felix Nieberding, Christian Wille, Yaoming Ma, Lukas Lehnert, Torsten Sachs
Data curation: Felix Nieberding, Christian Wille, Lukas Lehnert
Formal analysis: Felix Nieberding, Christian Wille, Lukas Lehnert
Funding acquisition: Yaoming Ma, Torsten Sachs

1. Introduction

During the 270 years since the beginning of the Industrial Era, the atmospheric carbon dioxide (CO_2) concentration has increased by ~50%, from 277 parts per million (ppm) in 1750 (Joos & Spahni, 2008) to more than 410 ppm in 2020 (Friedlingstein et al., 2020), reaching the highest level since at least 800,000 years. The increased CO_2 concentration is mainly caused by emissions from fossil fuel combustion, cement production and extensive land use change (Friedlingstein et al., 2020). These changes modify the radiation budget by increasing the amount of solar radiation that gets absorbed by the earth's surface and atmosphere, leading

Investigation: Felix Nieberding, Yuyang Wang, Philipp Maurischat, Lukas Lehnert, Torsten Sachs
Methodology: Felix Nieberding, Christian Wille, Philipp Maurischat, Lukas Lehnert, Torsten Sachs
Project Administration: Yaoming Ma, Torsten Sachs
Resources: Yaoming Ma, Torsten Sachs
Software: Felix Nieberding, Christian Wille, Philipp Maurischat, Lukas Lehnert
Supervision: Torsten Sachs
Validation: Felix Nieberding, Christian Wille
Visualization: Felix Nieberding
Writing – original draft: Felix Nieberding, Christian Wille, Lukas Lehnert
Writing – review & editing: Felix Nieberding, Christian Wille, Yaoming Ma, Yuyang Wang, Philipp Maurischat, Lukas Lehnert, Torsten Sachs

to the well-known greenhouse effect. As a response, the earth has warmed by roughly 1°C compared to the twentieth century average (NOAA National Centers for Environmental Information, 2021). The high and low latitudes, as well as the high mountain environments have experienced the biggest temperature increases and are thus especially vulnerable to global warming.

With an average elevation of more than 4,000 m above sea level (a.s.l.) and large numbers of glacial and periglacial land forms, the Tibetan Plateau (TP) was once called the Third Pole of the earth (Qiu, 2008). But how much longer will this be the case? Similar to the northern high latitudes, the TP is warming considerably faster than the global average. Since 1970 the air temperature has increased with roughly 0.35 C per decade (Yao et al., 2019). The rising temperatures have profound influences on the hydrological cycle: Melting glaciers, degradation of permafrost, increasing river discharge and rising lake levels are among the most prominent effects of global warming. Furthermore, the TP experiences increasing precipitation throughout most regions and times of the year (Wang et al., 2018; Yang et al., 2014). The topography, as well as the complex interplay between temperature and moisture availability determine the occurrence of the different ecosystems on the plateau (You et al., 2019). Nearly half of the plateau's surface is covered with the biggest pastoralist system in the world, comprised of 450,000 km^2 of *Kobresia pygmaea* (syn. *Carex parvula*) pastures and about 800,000 km^2 of alpine steppe ecosystems (Miehe et al., 2011, 2019). The Tibetan grasslands not only provide the livelihood for the (semi-) nomadic Tibetan herders to raise their livestock, they also store up to 3.3% soil organic carbon, thus being part of the global carbon cycle (Zhou et al., 2019). The short vegetation period, together with cold and dry winters leads to permanently low carbon turn-over rates, resulting in the accumulation of roughly 3.5 Pg C in the Tibet Autonomous region alone (Zhou et al., 2019).

The TP is characterized by strong diurnal and seasonal gradients of radiation, temperature and moisture availability. The majority of the observed warming trend, at about twice the mean annual trend, occurs during the winter months (Yao et al., 2019). Corresponding to the increase of the mean temperatures, the maximum and minimum temperatures increase as well. The minimum temperature increases more than the maximum temperature, which leads to a decrease in the daily temperature range (DTR) of 0.2°C per decade (You et al., 2016). The narrower DTR is explained by increasing low level cloud cover, which intercepts outgoing longwave radiation during nighttime and, to a smaller extend, blocks incoming solar radiation during the day (Duan & Wu, 2006). Another cause is the increased evaporation due to the higher soil moisture, which in turn is a consequence of increasing precipitation (Yang & Ren, 2017; Yang et al., 2011; You et al., 2016). As the surface becomes darker due to the increasing loss of snow and ice covered areas, it can absorb more solar radiation. The additional energy input heats up the surface, thus amplifying the role of the TP as mid-tropospheric heat source, which plays a crucial role in the timing and intensity of the Indian summer monsoon (ISM) (Ge et al., 2017). About 80% of the annual precipitation occur during the summer months from June to August and only about 10% during the winter months from December to February (Wang et al., 2018). Since the 1960s, precipitation has shown an average increasing trend of about 5.1 mm per decade (Wang et al., 2018). However, the increase in precipitation is unevenly distributed spatially and temporally. While the precipitation is increasing in the central, northern and southern TP, it is strongly decreasing in the eastern plateau and on the south-eastern periphery (Yang et al., 2014). The increase in precipitation takes place mainly in spring, while the other seasons only show slight but not significant increasing trends (Wang et al., 2018). The earlier onset of summer monsoon precipitation was found to play a major role in increasing lake areas of the endorheic inner TP (Liu et al., 2019), as well as in increasing soil moisture and a widespread greening of the ecosystems during early summer (Zhang et al., 2017). Several authors highlight that the observed changes in temperature and precipitation are responsible for advancing phenological trends, as well as summer greening in most regions of the TP (e.g., H. Wang et al., 2020; Li et al., 2019; Shen et al., 2011, 2016; Zhang et al., 2013).

The identification of the main drivers of ecosystem respiration and soil organic carbon stocks have been extensively investigated in the *K. pygmaea* pastures, which occur mostly on the central and eastern TP (e.g., Babel et al., 2014; Gu et al., 2003; Kato et al., 2004, 2006; Zhang et al., 2018; Zhao et al., 2017, 2018). With decreasing precipitation to the west, the *K. pygmaea* pastures are replaced by alpine steppe vegetation. The alpine steppe dominates wherever the *K. pygmaea* plants cannot form their typical mono-specific closed root mats, either due to lack of precipitation or overgrazing by livestock. Although the transition is associated with the loss of up to 70% of the SOC stocks (Miehe et al., 2019), at least the eastern alpine steppe

still contains up to 3.3% SOC (Zhou et al., 2019). However, it has received relatively little interest despite covering an area about twice the size of the *K. pygmaea* pastures.

The few studies which exist on ecosystem-atmosphere carbon cycling in the Tibetan alpine steppe ecosystems assign the inter-annual flux variability mainly to varying monsoonal precipitation (Wang et al., 2016, Y. Wang et al., 2020; Zhu et al., 2015). Y Wang et al. (2020) and Zhu et al. (2015) found the alpine steppe to act as a carbon sink during the growing seasons of dry and wet years but Wang et al. (2016) found a small net carbon source on an annual basis. It remains uncertain if the Tibetan alpine steppe ecosystem is currently a net sink or a net source of CO_2 and in which way the observed climate changes influence the carbon cycling. On the one hand, the warmer and wetter climate could enhance the autotrophic and heterotrophic soil respiration, thus increasing loss of carbon to the atmosphere. On the other hand, increasing temperature and precipitation are stimulating plant growth, thus enhancing carbon uptake through increased primary production (Chen et al., 2014). The difficult accessibility and harsh environmental conditions provide a challenging environment for conducting (micro-) meteorological measurements. Hence, most studies draw their conclusions only from observations during the growing seasons of a few years at most (e.g., Pei et al., 2009; Wei et al., 2012, 2014; Y. Wang et al., 2020; Zhu et al., 2015). The aim of this study is to disentangle the complex interplay of climatic variations and the ecosystem-atmosphere exchange of CO_2, from daily to monthly and annual to inter-annual time spans. The analyses of long term carbon fluxes, associated meteorological observations and plant cover estimates from a central Tibetan alpine steppe ecosystem allow the investigation of the following research questions:

1. Can the general trend of increasing temperatures and precipitation also be observed in the alpine steppe ecosystem at Nam Co?
2. How is the ecosystem-atmosphere exchange of CO_2 characterized on daily to monthly and annual to inter-annual time scales?
3. Do the observed changes in environmental variables promote or hamper plant productivity and soil respiration in the long run?

2. Methods

2.1. Study Site

The study site is located at the Nam Co Station for Multi-sphere Observation and Research (NAMORS, Chinese Academy of Sciences [CAS]), about 220 km north of the Tibetan capital Lhasa (30 46'N, 90 57'E). It is situated on a plain, sandy terrace between lake Nam Co (1 km NW) and the Nyainqêntanglha range (15 km SSE) at 4,730 m a.s.l. The climate is controlled by large-scale circulations and is therefore subject to strong annual variation. During winter, the prevailing westerlies provide cold air masses from central Asia. From December to February, the daily mean air temperatures stay below 0°C (minima below −20°C) with mostly clear and dry conditions. Usually, no closed snow cover is achieved for longer time periods, but in some years there can be heavy snowfalls (Wei et al., 2017). Therefore, the spring snow melt supplies only a small amount of moisture to the soil, which percolates quickly to deeper soil layers. The soil moisture then decreases until the ISM arrives, typically between May and June. From May to September, the humid air masses from the Bay of Bengal and the Arabian Sea provide about 80% of the annual precipitation, which ranges from 291 to 568 mm (mean = 403 mm). Between September and October, the weather gets colder and dryer again (Yao et al., 2013). The study site is situated in the transition zone between the *K. pygmaea* pastures and the dryer, less productive alpine steppe ecosystem. The alpine steppe at the NAMORS is characterized by *Stipa purpurea* but comprises further species from the families *Artemisia*, *Stipa*, *Poa*, *Festuca*, and *Carex* (Li, 2018; Miehe et al., 2011). Due to heavy grazing by yak, sheep and goat, the vegetation does not exceed 5 cm in height and a surface coverage of 50%. However, it is to note that the whole station was fenced in 2005, thus excluding the otherwise ubiquitous livestock grazing. Also in 2005, the Institute of Tibetan Plateau Research (ITP), CAS installed (micro-) meteorological measurements at the NAMORS (Ma et al., 2009). A 3 m Eddy Covariance tower measures the 3D wind vector with a CSAT3 ultrasonic anemometer and the carbon and water vapor fluxes using a Li-7500 open path infrared gas analyzer (IRGA). A 52 m planetary boundary layer tower (PBL) is equipped with air temperature and relative humidity measurements at 5 different heights (1.5, 2, 4, 10, 20 m) and measurements of wind speed and wind direction at 3 different heights (1.5, 10, 20 m). Additionally, the site is equipped with soil temperature

and soil moisture measurements (0, −10, −20, −40, −80, −160 cm). The soil moisture content is measured using time-domain reflectrometry (TDR) sensors. Because ice has a lower permittivity than liquid water, soil moisture measurements become unrealistically low during frozen conditions. Therefore, soil moisture measurements with soil temperature <0 C were discarded before aggregating to daily, monthly and annual averages. The station is furthermore equipped with measurements of soil heat flux (−10, −20 cm) and radiation (short and long wave downward and upward radiation, global radiation), precipitation and air pressure measurements. Since 2013, the station comprises a sensor measuring photosynthetic active radiation (PAR) (Zhu et al., 2015). For detailed information about the equipment and infrastructure, please see Ma et al. (2009, 2017).

2.2. Data Processing

2.2.1. Previous Work

In an earlier study, the authors of this manuscript published the fully processed and quality controlled EC flux data set from Nam Co (Nieberding et al., 2020). The 30-min averaged fluxes of CO_2, water vapor (H_2O), sensible and latent heat flux (H and LE, respectively) were calculated from the original 10 Hz EC measurements using the raw data processing software EddyPro (v7.0.6, LI-COR Inc.). Due to the remote location and harsh environmental conditions on the TP, sensor maintenance and calibration were performed irregularly, leading to a drift in mean CO_2 and H_2O concentration measurements. This drift was corrected by applying the offset between the measured CO_2 and H_2O concentrations and a reference time series to the raw 10 Hz measurements following Fratini et al. (2014). This way, the drift in concentration measurements was efficiently removed which prevented an overestimation of the mean carbon uptake by roughly 28%. During the course of the measurements, several buildings and scientific infrastructure were constructed close to the EC tower. Analyses of the wind direction distributions of wind speed and turbulent kinetic energy (TKE) suggest that the buildings do have some influence on the flow regime. Hence, fluxes originating from possibly disturbed wind sectors were completely excluded from further analyses. To get a more complete picture, the CO_2 flux data gaps were filled using the look-up table (LUT) approach provided in the REddyProc R package (Wutzler et al., 2018). Due to the harsh environmental conditions and the rigorous exclusion of possibly disturbed wind sectors, the overall data availability for Net Ecosystem CO_2 Exchange (NEE) after QC was only 28% (Figure 1).

2.2.2. Data Screening, Gap Filling and Flux Partitioning

The LUT gap filling procedure relies heavily on the availability of meteorological measurements (mainly air temperature, radiation and vapor pressure deficit). These variables are narrowly binned within certain time windows around the data gap in order to average the missing CO_2 flux values from available values during similar meteorological conditions and times (Wutzler et al., 2018). If not enough data points are available, the time window is successively widened until averaging is possible. Thus, the LUT procedure replicates the existing flux values before and after the data gap causing a greater uncertainty the larger the data gap is. Hence, we decided to modify the quality filtering of our previous study to make the gap filling procedure more robust by obtaining as much physiologically plausible data as possible.

First, we relaxed the wind direction filtering. In our previous study, we preemptively excluded all fluxes from possibly disturbed wind sectors, even though only the main building exerts a clear influence on the quality of the fluxes. This led to the exclusion of roughly 20% of all measured data points. Now we exclude only those wind sectors that are clearly disturbed, namely the two-storey main building and the back of the CSAT3 ultrasonic anemometer. Furthermore, an analytic approach was applied to exclude implausible measurements of night time carbon uptake while accounting for the seasonal variation of fluxes and flux noise. Originally, we rigorously excluded night time fluxes <-0.1 mol m^{-2} s^{-1} to discard unreasonable fluxes while allowing some variability in the data. Now, the cut-off threshold was estimated for every month individually by fitting a tangent to the density curve of night-time CO_2 fluxes at the point where the first derivative of the density curve has its maximum. The intercept of this tangent with the x-axis is then taken as cut-off threshold. The threshold is set to 0 mol m^{-2} s^{-1} if it was found to be >0 mol m^{-2} s^{-1}. This way, physiologically implausible measurements were discarded while allowing the typical flux variability around the

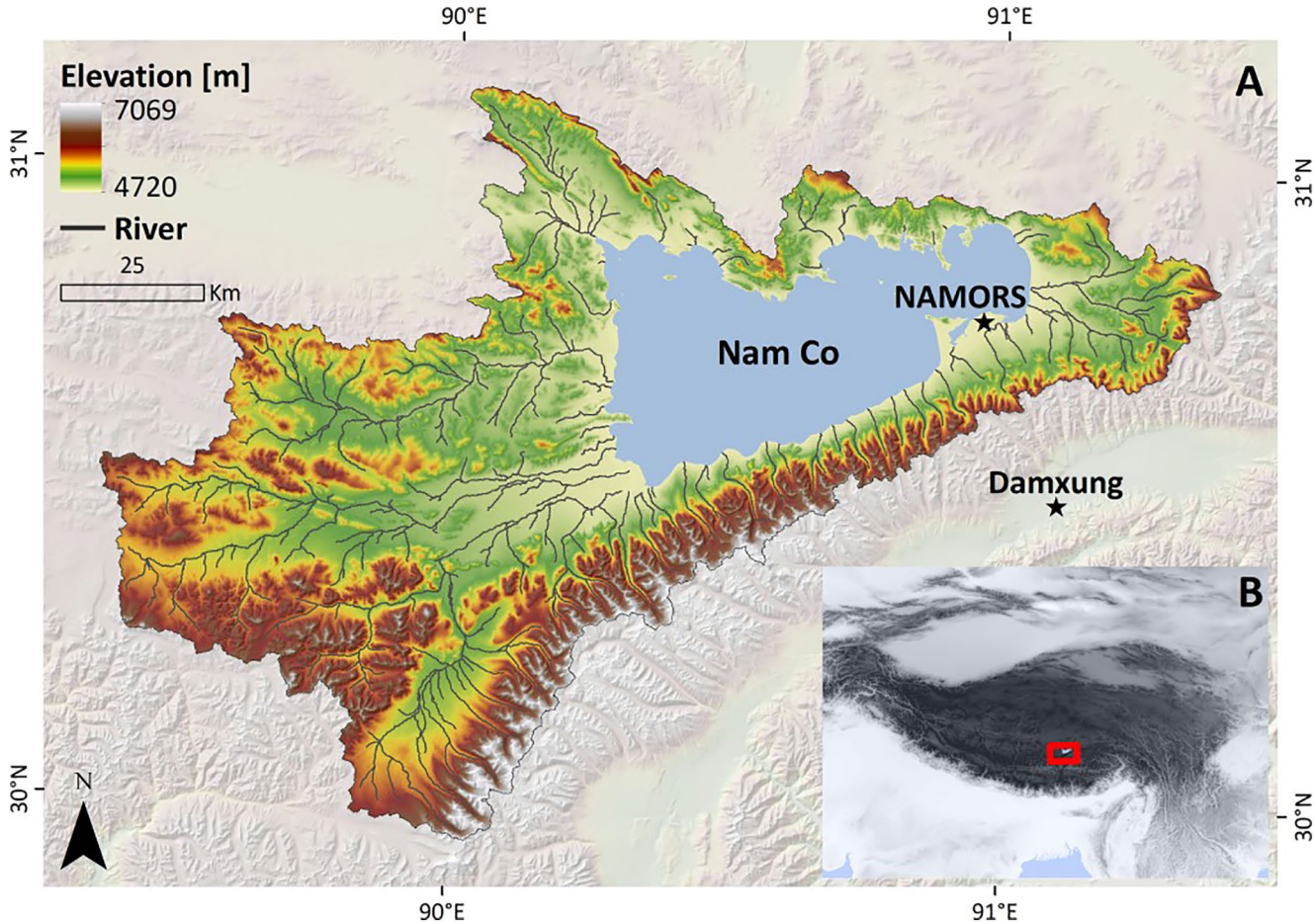

Figure 1. (a) Surface elevation of the Nam Co catchment according to SRTM v4 (Jarvis et al., 2008), the Nam Co lake extent based on a supervised classification of Sentinel-2 imagery of January 30, 2018 (JAXA; Copernicus Sentinel data (2018) processed by ESA; Jarvis et al., 2008) and river systems based on ALOS surface elevation, generated by Laura Keys (JAXA — Japan Aerospace Exploration Agency). (b) Surface elevation of the Tibetan Plateau indicating the location of the Nam Co (JAXA; Copernicus Sentinel data (2018) processed by ESA; Jarvis et al., 2008).

mean. The calculations can be found in the R scripts and monthly plots illustrating the process are provided in the supporting information (Figures S1–S12).

Building on our previous work, we also enhanced the gap filling of meteorological variables. As mentioned in Section 2.1, there are usually several measurements of the same variable available. For air temperature (Tair) and relative humidity (rH) there are measurements from 1.5, 2, 3, 4, 10, and 20 m available, which originate from the two different towers (EC and PBL). Similarly, soil temperature (Tsoil) and soil moisture (SMC) measurements exist from 0, 10, 20, 40, 80, and 160 cm depth. Incoming solar radiation (Rg) data exists from 3 independent devices which measure shortwave incoming radiation (Kipp & Zonen CNR1 and CMP11) and PAR (Apogee Original Quantum Sensor). Based on annual linear regression, the different measurements were combined to one overall time series. The most reliable time series closest to the ground was used as starting variable which was then iteratively gap-filled with the ones having the highest linear regression coefficient R^2. Vapor pressure deficit (VPD) was calculated from the gap-filled time series of Tair and rH. Remaining short data gaps of up to two time steps were filled using linear interpolation. Following the procedure from our previous manuscript, we applied the quality control scheme for CO_2 and H_2O fluxes also to the flux measurements of H and LE. Finally, the LUT method from REddyProc was used for gap filling of the fluxes and meteorological variables.

The measured CO_2 fluxes represent the NEE, which we partitioned into its components gross primary production (GPP) and ecosystem respiration (Reco), representing the photosynthetic uptake of CO_2 and

the autotrophic and heterotrophic soil respiration, respectively. We use the day time partitioning approach within REddyProc to model GPP and Reco (Lasslop et al., 2010; Wutzler et al., 2018). Please note that GPP and Reco are estimated individually and therefore do not necessarily add up exactly to NEE. The final 30-min time series of the fluxes and meteorological variables were aggregated to daily, monthly and annual estimates (Reis & Ribeiro, 2020).

2.3. Resource Use Efficiency

To get a wider picture of the mass-energy exchange between the alpine steppe ecosystem and the atmosphere, we calculated different resource use efficiencies. As we are using Eddy Covariance measurements, our estimates of water use efficiency (WUE) and light use efficiency (LUE) represent whole ecosystem estimates, rather than the oftentimes used resource use efficiencies at the plant level. Ecosystem LUE (g C MJ^{-1}) was calculated as the ratio of *GPP* (g C m^{-2} $time^{-1}$) to incoming shortwave radiation (MJ m^{-2} $time^{-1}$):

$$LUE = \frac{GPP}{Rg} \tag{1}$$

Ecosystem WUE (g C mm^{-1} H_2O) was calculated as the ratio of *GPP* (g C m^{-2} $time^{-1}$) to evapotranspiration (*ET* in mm $time^{-1}$)

$$WUE = \frac{GPP}{ET} \tag{2}$$

where *ET* was calculated from latent energy flux (LE in W m^{-2}) and air temperature (Tair in °C) following Equation 65 in Reis and Ribeiro (2020):

$$ET = \frac{1.8}{2500 - 2.37 * Tair} * LE \tag{3}$$

ET was calculated for every half hourly time step and then summed up to daily or monthly values.

2.4. Trend Analysis

When analyzing such a long data set, the question arises as to whether a trend exists and how this might be related to the profound environmental changes of the recent decades. The non-parametric Mann-Kendall (MK) test is widely applied in the detection of monotonic trends in hydro-meteorological time series because it has no requirements of homoscedasticity or prior assumptions of the sample distribution (F. Wang et al., 2020). The MK test statistic is determined by the ranks and sequences of a time series rather than the original values. It is robust against outliers, missing values and non-normally distributed data. However, the MK test assumes that the data are independent and randomly ordered. Hence, it is not robust against serial auto-correlation as it is frequently encountered in hydro-meteorological time series. A positive auto-correlation in the time series may lead to Type I errors, i.e., detecting a trend where none exists. Hamed and Rao (1998) developed an empirically determined correction factor to modify the variance of the MK test statistic (hereafter called MMKH). While this method can reduce the effect of serial correlation, it will lead to an increase in Type II errors (i.e., rejection of a trend where one exists) if a trend is present in the data (Yue & Wang, 2002; Yue et al., 2002). To overcome these shortcomings, Yue and Wang (2004) proposed to remove an existing trend prior to the estimation of the auto-correlation coefficients from the the original data, rather than from the ranks of sample data (hereafter called MMKY). As pointed out by several studies (e.g., Blain, 2013; F. Wang et al., 2020), neither the original Mann Kendall test, nor its variance correction approaches can be used as a "silver bullet" for trend detection. The proposed methods have either problems preserving the adopted significance level (Type I error) or they are less powerful (Type II error). Hence, we performed both modified MK tests using "modifiedmk" library in R programming environment (Patakamuri & O'Brien, 2020).

Because the data gaps are irregularly distributed within the individual years, any trend test may lead to erroneous results when applied to the whole time series. While there are only few years without data gaps, there are usually more complete months available. Hence, the modified MK tests were performed using daily fluxes, meteorological variables and resource use efficiencies which were pooled on a monthly basis. Only months with >30% measured values after quality filtering and 100% data availability after gap filling were used. This ensures comparability between the years and accounts for uncertainties which may be

introduced when filling long data gaps. We report the *p*-values of both modified MK tests and treat them equally in our analysis. However, exceeding a certain significance level should not be used alone for binary hypothesis testing or model interpretation (Wasserstein & Lazar, 2016; Wasserstein et al., 2019). Hence, we also calculate Sen's slope, which is the median of the slopes of all linear regression lines through each pair of points (Sen, 1968). Since this slope estimation is stable against outliers, we get a more robust estimate of the effect size and can ultimately draw conclusions about the relevance of our results. The exact *p*-values of both modified MK tests and the Sen's slope estimations are provided in the supporting information (Tables S1–S3).

2.5. Plant Cover

We estimated annual plant coverage for the area close to the NAMORS using the pre-trained support vector machine regression (SVM) models published in Lehnert et al. (2015). These are fully validated against field samples of the five major grassland types found on the TP: (1) *Kobresia pygmaea* pastures, (2) *Kobresia humilis* pastures, (3) swamps and salt marshes, (4) montane, and (5) alpine steppes. With an overall RMSE of ≤7%, SVM showed the best performance compared to three other regression models. For our study site, the SVM models were applied to multispectral satellite data acquired by Landsat 5, 7, and 8 at 30 m spatial resolution (downloaded from USGS EarthExplorer). The Landsat scenes were processed using an extended version of the 6S code for atmospheric correction (Curatola Fernández et al., 2015; Vermote et al., 1997) and the Minnaert model for topographic corrections (Riano et al., 2003). The data was filtered for obstructions (e.g., clouds) using the quality bands shipped with the Landsat data. Therefore, a scene listed in the EarthExplorer with a high cloud cover percentage that had clouds distributed over lake Nam Co rather than the mountain ranges to the south was chosen over a scene with a lower listed cloud cover with non-optimal cloud distribution. In addition, if both Landsat TM and Landsat ETM + images were available for a year, TM scenes were chosen over ETM + scenes if there was no remarkable difference in cloud distribution. To ensure full development of plant coverage and hence comparability between the years, only Landsat scenes acquired during the summer months (JJA) were used. During the study period from 2005 to 2020, a total of 14 catchment-wide acquisitions were available for the plant cover assessment. If multiple cloud-free scenes acquired during the summer months were available for one year, the scene acquired closest to fifteenth of July has been selected. Pixel-wise mean and standard deviations of plant coverage were calculated and the final product was cross-verified by post hoc assessment of the field investigation. For the trend analysis, the same modified non-parametric Mann-Kendall correlation tests following Hamed and Rao (1998) and Yue and Wang (2004) were applied on a pixel based approach. Only pixels with at least 9 valid plant cover estimates were used to detect changes of plant cover over time (at 95% significance level). In the following, we will use the term greening to refer to a significant increase in plant cover.

3. Results

3.1. Climate Variability

Daily and monthly variation in the major environmental variables are shown in Figure A1 and Table 1. All variables reflect the strong annual variation which not only follows the insolation but is also subject to the large scale circulation patterns, namely the ISM and the westerlies during winter. Solar radiation, representing the main heat source on the Plateau peaks in May, just before the arrival of moist air masses and the associated increase in cloud cover. While Tair and surface Tsoil follow the basic annual insolation pattern, there are remarkable differences between them. The average annual soil temperature is more than 5 C higher than the average annual air temperature. This is true for every month but especially pronounced during summer. The largest differences occur in May and June, where the average Tsoil is more than 8 C warmer than the average Tair. The lowest values occur between December and February with mean temperatures well below freezing point. The mean annual precipitation is roughly 400 mm but the inter- and intra-annual variability is high. Annual precipitation sums range from 295 mm in 2006 to 569 mm in 2010. More than 80% of the mean annual precipitation occur between May and September and less than 4% occur between November and March. While the relative air humidity follows the annual precipitation distribution quite fast, there is a delay in soil moisture, with highest values between July and October. However, with a maximum daily average water content of 37%, soil moisture remains quite low throughout the year. Vapor pres-

Table 1
Average Monthly Meteorological Variables and Fluxes

	Tair	Tsoil	Rg	VPD	SMC	rH	PPT	NEE	GPP	Reco	H	LE
Month	°C	°C	MJ m^{-2}	hPa	%	%	mm	g C m^{-2}	g C m^{-2}	g C m^{-2}	W m^{-2}	W m^{-2}
Jan	−10.8	−8.3	452	2.0	2.2	40	3	−2.4	16.0	8.4	9.1	10.2
Feb	−9.9	−5.9	496	2.0	2.4	44	1	−6.8	15.9	6.6	26.6	9.1
Mar	−6.3	−1.0	697	2.5	5.3	44	3	−11.4	22.6	7.9	46.0	13.6
Apr	−1.6	5.7	780	3.2	4.7	50	12	−12.6	27.9	11.2	60.5	18.2
May	3.0	11.4	856	3.9	4.9	57	20	−12.8	36.3	18.9	66.2	31.1
Jun	7.7	16.2	801	4.8	5.7	60	37	−20.6	44.2	27.1	58.8	51.1
Jul	9.1	15.3	727	4.3	9.5	67	87	−19.5	55.2	42.2	39.2	68.1
Aug	8.4	13.5	679	4.0	11.7	68	111	−19.5	58.7	44.2	33.9	65.1
Sep	6.3	10.5	597	3.8	12.0	65	81	−14.9	40.7	29.5	27.7	64.8
Oct	0.3	3.7	572	3.4	9.6	55	36	−3.5	21.9	13.4	21.0	33.2
Nov	−6.3	−2.6	478	2.5	4.7	45	7	−0.5	13.4	7.6	5.1	14.7
Dec	−8.2	−6.0	425	2.4	2.2	38	1	−3.0	13.2	6.6	9.4	8.5
Total	−0.7	4.4	7,560	3.2	6.2	53	398	−127.5	366.0	223.6	33.6	32.3

sure deficit peaks during early summer and stays relatively high until September. The lowest VPD values of 2 hPa occur during January and February. More detailed tables including minimum and maximum air and soil temperatures, as well as the respective standard deviations for the average values shown in Table 1 can be found in the supporting information (Tables S4 and S5).

3.2. Seasonal Course of Fluxes

Following the usual micrometeorological convention, negative values for NEE, H and LE represent fluxes toward the surface and positive values represent fluxes away from the surface. Note that while GPP and Reco are both positive, GPP represents carbon uptake and Reco represents carbon release. Table 1 shows the monthly average, and Figure 2 shows the daily average carbon and heat fluxes throughout the whole study period. Between November and January, daily NEE remains close to zero. Beginning in February, NEE becomes more and more negative and reaches a maximum monthly carbon uptake of ≥19 g C m^{-2} month^{-1} during June, July, and August. Between September and October, carbon uptake decreases rapidly back to values close to zero. GPP and Reco show a somewhat different pattern with a maximum during August and rapid decline afterward. Interestingly, both variables indicate biological activity even during the cold and dry winter months December to February. The sensible and latent heat fluxes show a complimentary behavior, following the strong annual seasonality on the TP. The sensible heat flux peaks already in May, right before the onset of summer monsoon precipitation and cloud cover. Correspondingly, the strongest latent heat fluxes occur from July to September, when water availability is highest.

3.3. Trend Analysis

The results of the two different modified MK tests (MMKH and MMKY, Figure 3) show a significant increase of the CO_2 sink strength during all months. In September only MMKY indicates a significant trend whereas during all other months, both tests yield statistically significant trends. The months of May, June, and July exhibit the strongest increase in daily carbon uptake with −1.3, −0.7, and −1.0 g C m^{-2} decade^{-1}, respectively. The smallest changes of NEE were found for the months August, September and February. When averaged over the whole year, the daily carbon sink strength increased by 0.5 g C m^{-2} decade^{-1}. When looking at the partitioned fluxes, a distinct pattern becomes visible: During the months November to July, GPP and Reco generally increased, whereas during August to October GPP and Reco generally decreased. In the first case, GPP increased stronger than Reco while in the second case the decrease in GPP was less than

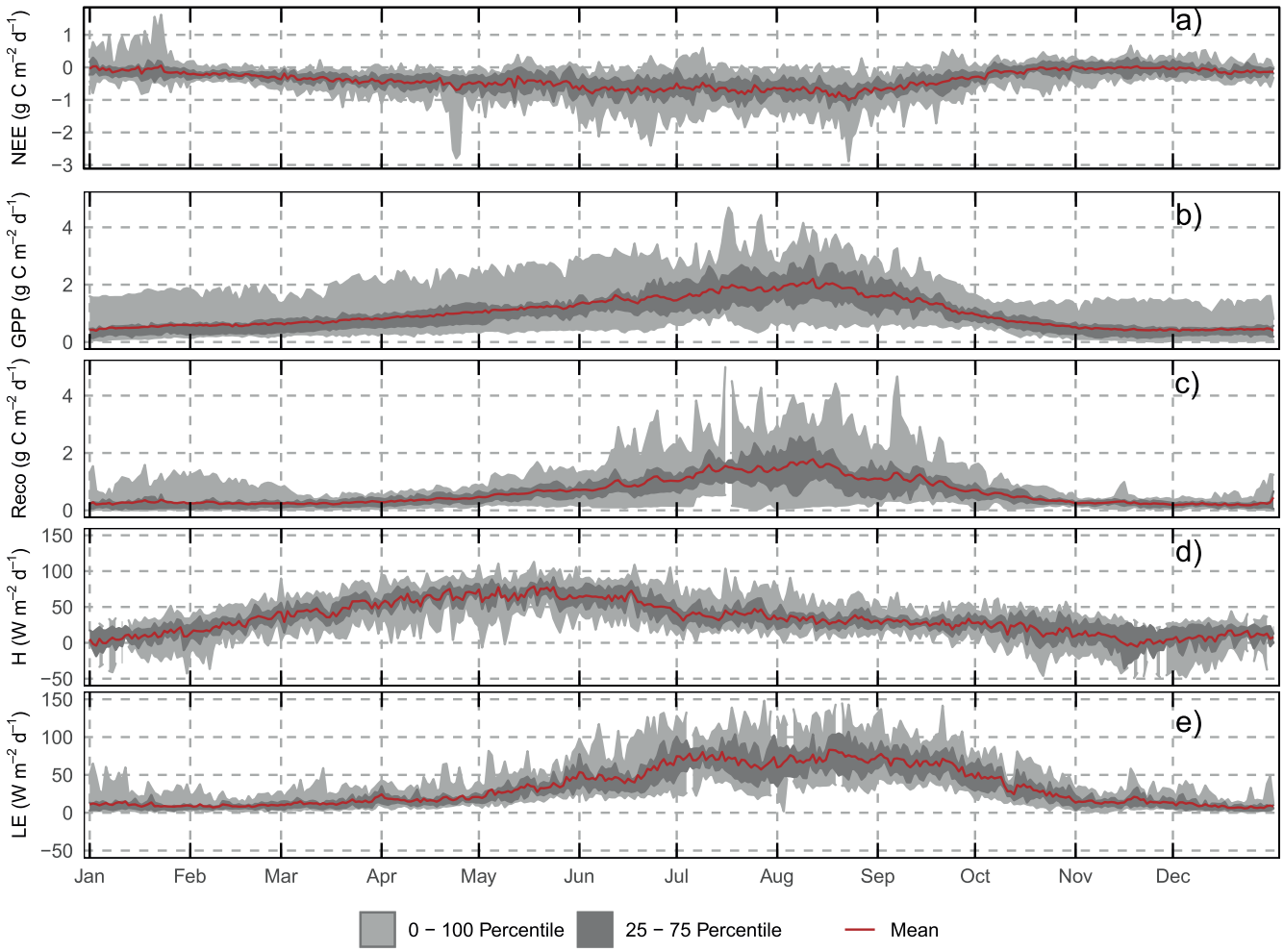

Figure 2. Mean annual course of all pooled years (2006–2019) of (a) net ecosystem exchange (NEE), (b) gross primary production (GPP), (c) ecosystem respiration (Reco), (d) sensible heat flux (H) and (e) latent heat flux (LE), as well as the 0–100 and 25–75 percentiles.

that of Reco, leading to the overall increasing carbon sink strength. On average, the daily GPP is increasing by 0.4 g C m^{-2} decade^{-1} but no overall trend was found for Reco. As the carbon fluxes are governed by the availability of light, heat and moisture, any changes in these variables can have diverse effects. The main changes during different periods of the year are as follows:

1. During November to February, we found a decrease of rH and LE and an increase of VPD which indicates a lower water availability. This very likely led to a change of the partitioning of available energy, away from LE and towards an observed increase of H. A strongly increasing diurnal soil temperature range can be observed (>10°C), with increasing maximum and decreasing minimum soil temperatures. The air temperatures do not exhibit such a clear trend but when averaged over the four months, we still see slightly increasing Tair mean, max and DTR and slightly decreasing Tair min. Figure 5 indicates that, during November to February, increasing maximum and minimum soil temperatures have opposite effects on NEE. Higher maximum soil temperatures increase carbon uptake while higher minimum soil temperatures increase carbon release.
2. During early summer, daily light availability is strongly decreasing with −2.3 and −1.3 MJ m^{-2} decade^{-1} during June and July, respectively. With significantly decreasing H and Tsoil (mean, max and DTR), heat availability is following this trend, especially at the surface. At the same time, higher moisture availability is indicated by increasing SMC and rH and lower VPD.
3. Especially during August but also during September to October, lower moisture availability is indicated by decreasing LE, and rH while VPD exhibits a positive trend. At the same time, Tair mean starts to in-

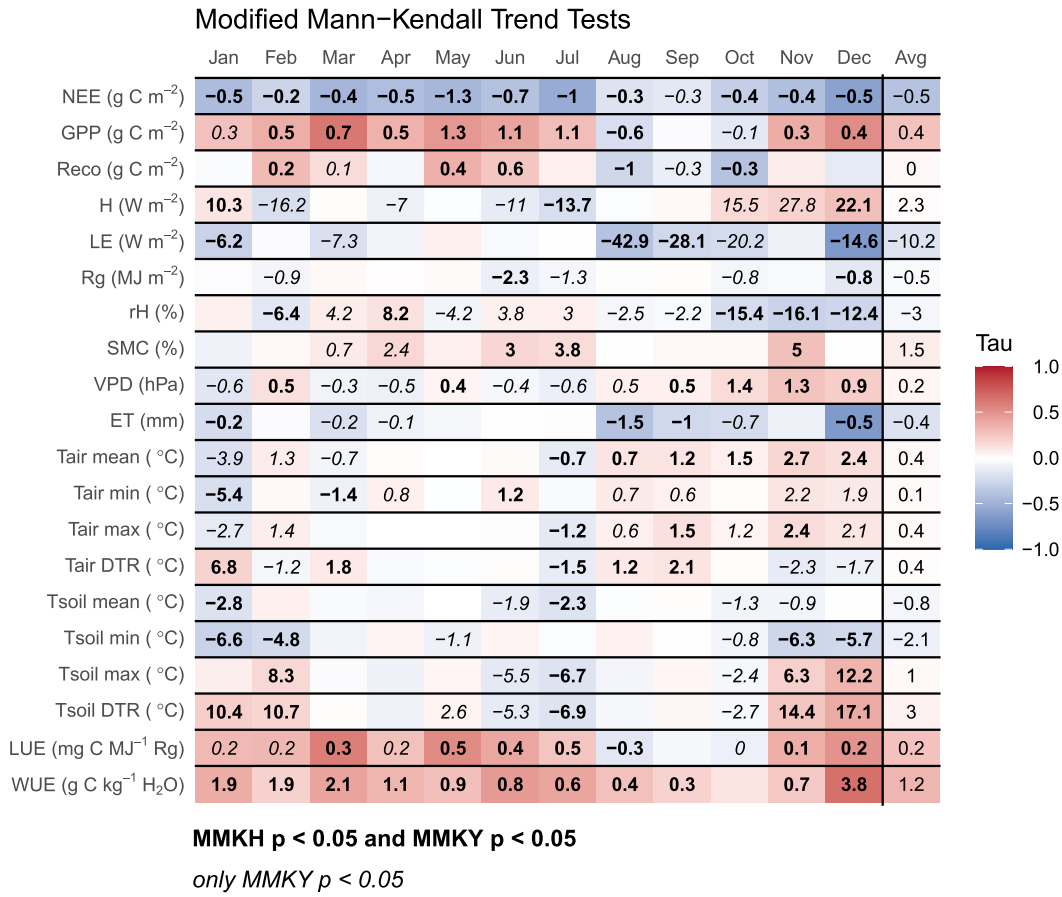

Figure 3. Modified Mann-Kendall trend test after Hamed and Rao (1998, MMKH) and Yue and Wang (2004, MMKY). The numbers represent the effect size in native units per decade (Sen's slope). They are written in bold if both, MMKH and MMKY yielded a significant trend (p-value <0.05), in italics if only MMKY yielded a significant trend and no numbers are printed when both tests were insignificant. The relative effect strength (Kendall's Tau) is color coded from blue to red (−1–1). The column Avg represents the mean Sen's slope and Tau of all significant and non-significant months.

crease and also air DTR is increasing, mostly due to stronger increases in Tair max than in Tair min. The drying trend is also supported by Figure A2, which shows decreasing monthly precipitation sums during August (−6.26 mm yr^{-1}) and September (−2.15 mm yr^{-1}).

The other months do not show any trends in precipitation, but it is to note that variability is quite high between the years, especially during the summer months. Because precipitation is a discontinuous phenomenon, it was not included in the modified MK trend test. The many days with zero precipitation and the broadly distributed precipitation events would not be covered adequately by the test statistics.

The water use efficiencies show a consistent increase throughout all months (Figure 3), with the strongest effect from December to March. The LUE is also increasing during most times of the year with the highest increases from May to July whereas a negative, yet not always significant trend can be observed between August and October. For the summer months it becomes clear, that the LUE is negatively correlated with H, Rg and VPD and positively correlated with LE, rH and SMC (6). The highest LUEs are observed at intermediate temperatures of 5–10 C and 10–15 C for Tair and Tsoil, respectively.

3.4. Plant Cover

The alpine steppe ecosystem around the NAMORS station exhibits mean plant covers of 30%–50% (Figure 4a). The area that is covered by the footprint of the EC system has a mean plant coverage of less than

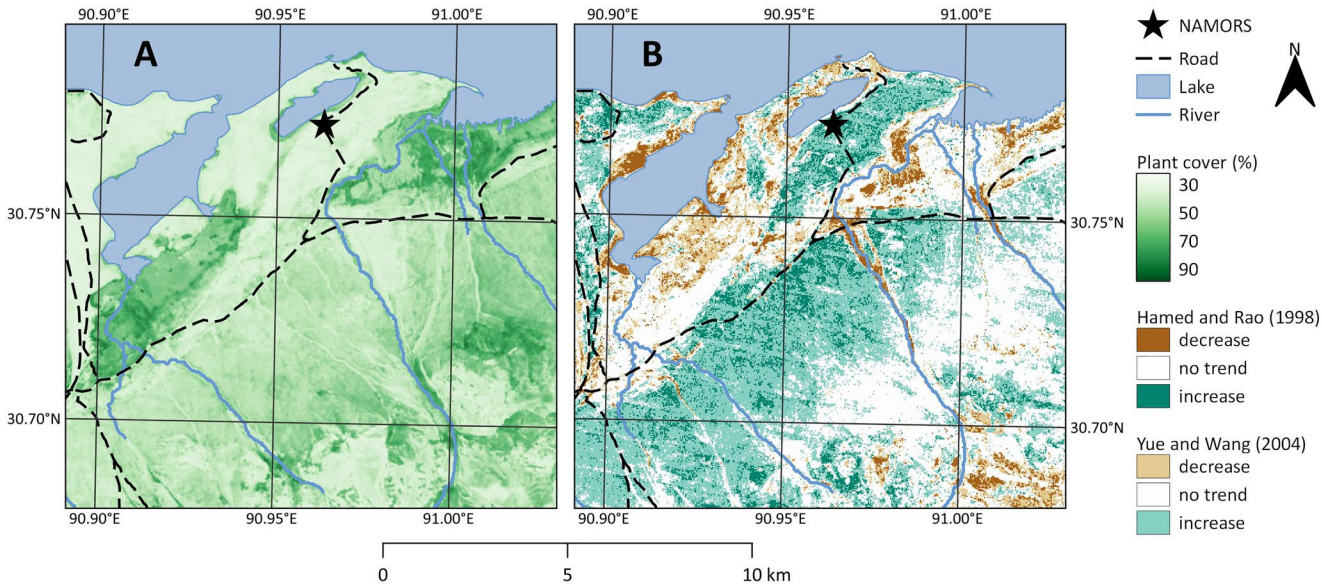

Figure 4. (a) Mean plant cover between 2005 and 2020 from the area close to the Nam Co Station for Multi-sphere Observation and Research (NAMORS) (30 46'N, 90 57'E) and (b) results of the modified Mann-Kendall trend tests after Hamed and Rao (1998) and Yue and Wang (2004) for the same area. Only statistically significant (p-value < 0.05) increasing or decreasing pixels are shown. Nearly all pixels that are significant for Hamed and Rao (1998) are also significant for Yue and Wang (2004). The SE to NW oriented "stripes" result from the failure of the Landsat 7 sensor in 2003, which led to missing data and consequently causes fewer samples to be available in the areas affected by the sensor failure. The decreased sample size yields slightly different trends and less significant pixels in these areas.

40%. There are areas to the south east and south west that show higher plant coverage up to 80%. These areas are mostly situated in depressions with continuous water availability from streams. The trend analysis (Figure 4b) shows a large scale greening of the alpine steppe ecosystem that is not only evident for the area close to the NAMORS but also for larger areas of alpine steppe ecosystems more to the south. The more productive areas at lower elevation exhibit a rather decreasing plant cover. As expected from theory (Section 2.4), MMKH indicates less significant trends than MMKY. If there is a significant trend in MMKH, it is almost always significant in MMKY as well. The tests only differ in the number of significant trends, not in the relative effect strength, nor the direction of the trend.

4. Discussion

4.1. Cold-Season Carbon Uptake

As already stated in our previous work, we find a diurnal pattern of carbon uptake and release even during the coldest months when air temperatures remain continuously below freezing point (Figure A3). However, due to the strong radiation and clear sky conditions, the soil heats up well above zero degrees, facilitating plant and soil microbial activity (Nieberding et al., 2020). While the temperature is sufficiently high, the availability of water for the biological activity remains unclear. The measured soil moisture content during December to February is typically below 5%. However, the dominant plants in the Tibetan alpine steppe such as *Stipa purpurea* are highly adapted to drought stress, for example, by regulating stomatal conductance (Yang et al., 2015). This enables the plants to maintain photosynthesis even under prolonged drought conditions. A possible, as yet unquantified, source of water could be dew and hoarfrost. This could form regularly at night during clear sky conditions on the TP and be taken up efficiently by the plants in the morning, before entering the soil and being detected by the soil moisture sensors. Groh et al. (2018) found dew and hoarfrost contributing substantially to the water budget at two humid low mountain grasslands in Germany, accounting for up to 38% of the total monthly precipitation amount, especially during winter months. Guo et al. (2016) estimated that dew formation contributed 7.2% of the corresponding rainfall amount to the growing season water availability in a cold desert-shrub ecosystem in Ningxia, NW China (1,530 m a.s.l).

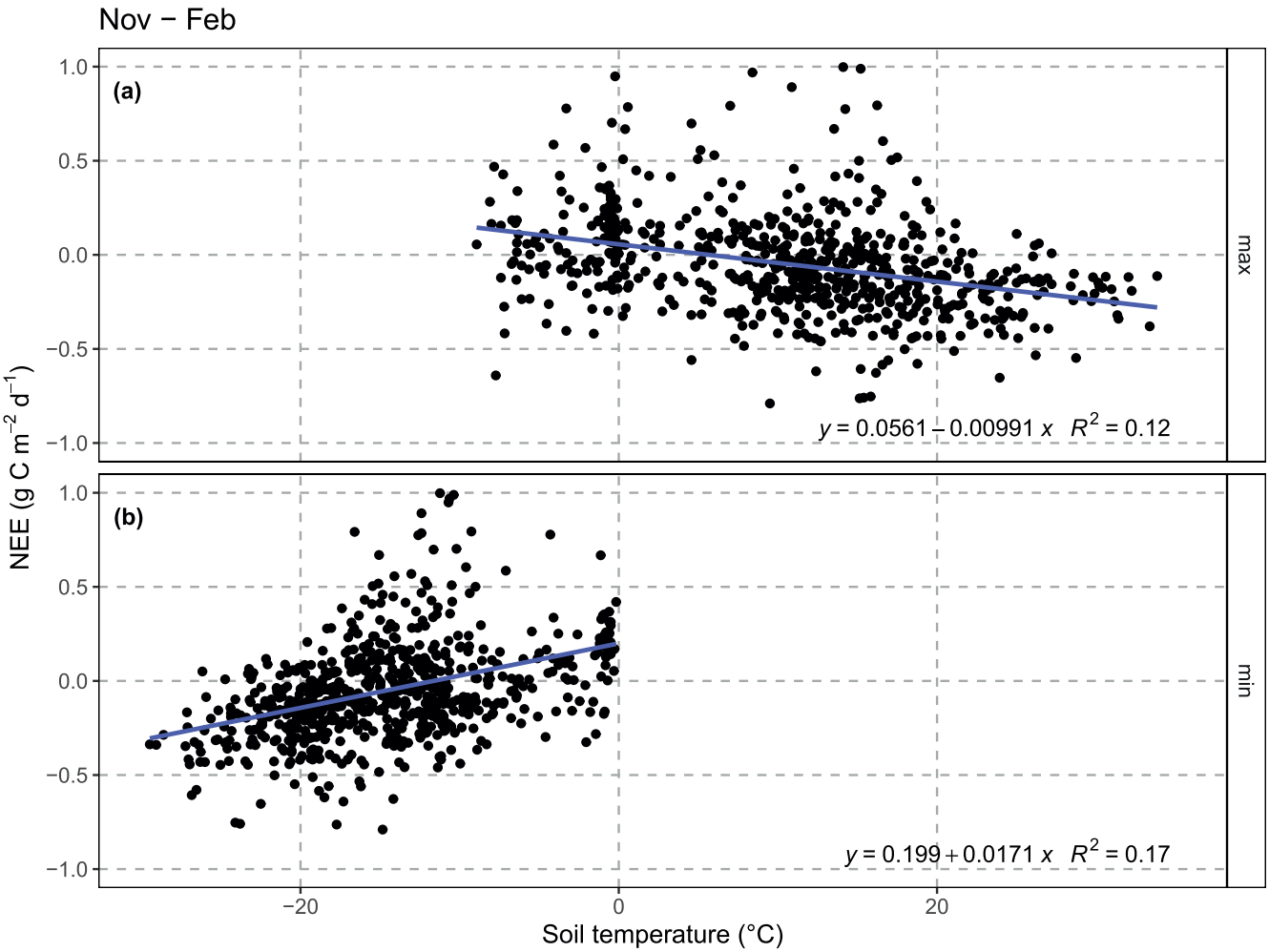

Figure 5. Relationship of daily (a) maximum and (b) minimum soil temperature with Net Ecosystem CO_2 Exchange (NEE) balance between November and February, using only months with >30% data availability.

To further test our hypotheses, in situ measurements of dew and hoarfrost formation are required by which their relevance for plant metabolic activities can be assessed, especially during the winter months.

4.2. Differential Effect of Soil Temperature on GPP and Reco

Between November and February, a strong increase of the diurnal soil temperature range of >10 C per decade was measured, caused by the combination of increasing daily maximum Tsoil and decreasing daily minimum Tsoil. Soil respiration is happening at night and during daytime, while carbon uptake is only possible at daytime through photosynthesis. An increase of daytime soil temperatures (Tsoil max) will increase both GPP and Reco while a decreasing night time temperature (Tsoil min) will only decrease soil respiration (Figure 5). Hence, both affect the carbon sequestration capacity toward higher carbon uptake, which is reflected by increasing GPP but a more or less steady Reco (Figure 3). An increasing DTR during December–January (1979–2012) was also reported by Yang and Ren (2017) for our study site at 30°N, 90°E while most other parts of the TP exhibit decreasing DTRs. The overall decreasing DTR was also found by other studies, which assign a stronger increase in minimum temperatures than in maximum temperatures to enhanced nighttime cloud cover (e.g., Duan & Wu, 2006; Yao et al., 2019). Hence, these seemingly contradictory findings actually highlight that the great spatial and temporal climatic variability throughout the TP has to be taken into account for studies on carbon, energy and water cycling.

4.3. Greening and Water Availability

Over the past decades, an advancing spring green-up date (GUD) has been reported for the TP grasslands by many authors (e.g., Zhang et al., 2013; Zheng et al., 2016). For the months March and April, we observed an increase in carbon uptake and a slightly increasing Reco, which agrees well with Li et al. (2019), who found that decreasing minimum temperatures in January and increasing minimum temperatures in spring fulfill the winter chilling and spring heat accumulation requirements earlier, thus promoting an earlier GUD. In the meantime, we found that both WUE and LUE in March increased. This can be a consequence of earlier GUD indicating that plants can use the available water and light resources more efficiently if they sprout earlier.

For the months May, June, and July, we found the strongest increase in carbon uptake and partly also in ecosystem respiration. For June and July it becomes clear that lower incoming shortwave radiation decreases soil temperatures during daytime, which also decreases Tsoil mean, Tsoil DTR and the sensible heat flux. While the increasing rH and decreasing VPD could be a result of the lower air temperatures, SMC clearly indicates higher water availability. However, the monthly precipitation sums do not show any increasing trend (Figure A2). Together, these changes are a consequence of increased cloud cover during the early summer months reducing the heat availability at the surface. No long term change is observed in LE during May to July, indicating that the effects of reduced energy availability and increased water availability roughly balance each other out.

Unlike during the other months, the increase in carbon uptake during late summer (August and September) is mainly caused by a decreasing daily Reco of up to -1 g C m^{-2} $decade^{-1}$, which roughly doubles the amount of the GPP decrease. August and September are also the only months with decreasing precipitation sums (-6.26 and -2.15 mm yr^{-1}, respectively). Together with increasing Tair and VPD and decreasing LE and rH, these variables indicate an enhanced drought situation during the late growing season.

The strongly increasing LUE between May and July and the decreasing LUE between August and September indicates that radiation, as well as heat and drought stress influence the ability of the alpine steppe to efficiently use the available light for photosynthesis. The increasing cloud cover during June and July is expected to decrease the amount of direct radiation and increase the amount of diffuse radiation (Huang et al., 2014). Diffuse radiation has a lower tendency to cause canopy photosynthetic saturation, resulting in higher light use efficiencies by the plant canopy (Gu et al., 2002; Zhu et al., 2015). On the contrary, increasing drought conditions during late summer may trigger stomatal regulation of the *S. purpurea* steppe, especially during noon when VPD and temperature are high (Körner, 1995; Yang et al., 2015; Zhu et al., 2015). These findings are corroborated by the positive correlation between LE, rH, and SMC with LUE during May to September (Figure 6). At the same time, H, Rg, and VPD exhibit a negative correlation with LUE, highlighting the sensitivity of plant productivity to shifting climatic patterns.

The special location of the study site just south of the large water masses of Nam Co leads to the formation of a regular lake-land breeze system (Biermann et al., 2014; Dai et al., 2020; Gerken et al., 2014). When the moist air masses from Nam Co get uplifted along the Nyainqêntanglha range to the south, deep convection gets triggered frequently due to adiabatic cooling and mesoscale circulation patterns (Gerken et al., 2015). Hence, the plain and the mountains south of Nam Co are preferential areas for cloud formation and precipitation. Any changes affecting either the land (like greening or pasture degradation) or the lake (e.g., warming, expansion) may affect local circulation patterns and hence cloud formation (Babel et al., 2014; Dai et al., 2020). However, Ma et al. (2016) found that evaporation of Nam Co exhibits a decreasing trend of -12 mm yr^{-1} between 1998 and 2008. These findings are consistent with our estimations, which exhibit an average -0.37 mm $decade^{-1}$ decrease of the daily ET for the alpine steppe ecosystem.

The NAMORS station was fenced in 2005, thus excluding the otherwise ubiquitous grazing by yak, sheep and goat. The absence of large grazers is expected to increase the above- and below-ground organic carbon content, which could also lead to the observed increase in CO_2 uptake (Liu et al., 2020). For our study site, we estimated that about 50%–60% of the fluxes originate from within the fenced area. Hence, the reported increase in carbon uptake is representative for the steppe ecosystem inside, as well as outside the fenced area. When taking the trends in plant cover (Figure 4) into account, it becomes obvious that the observed

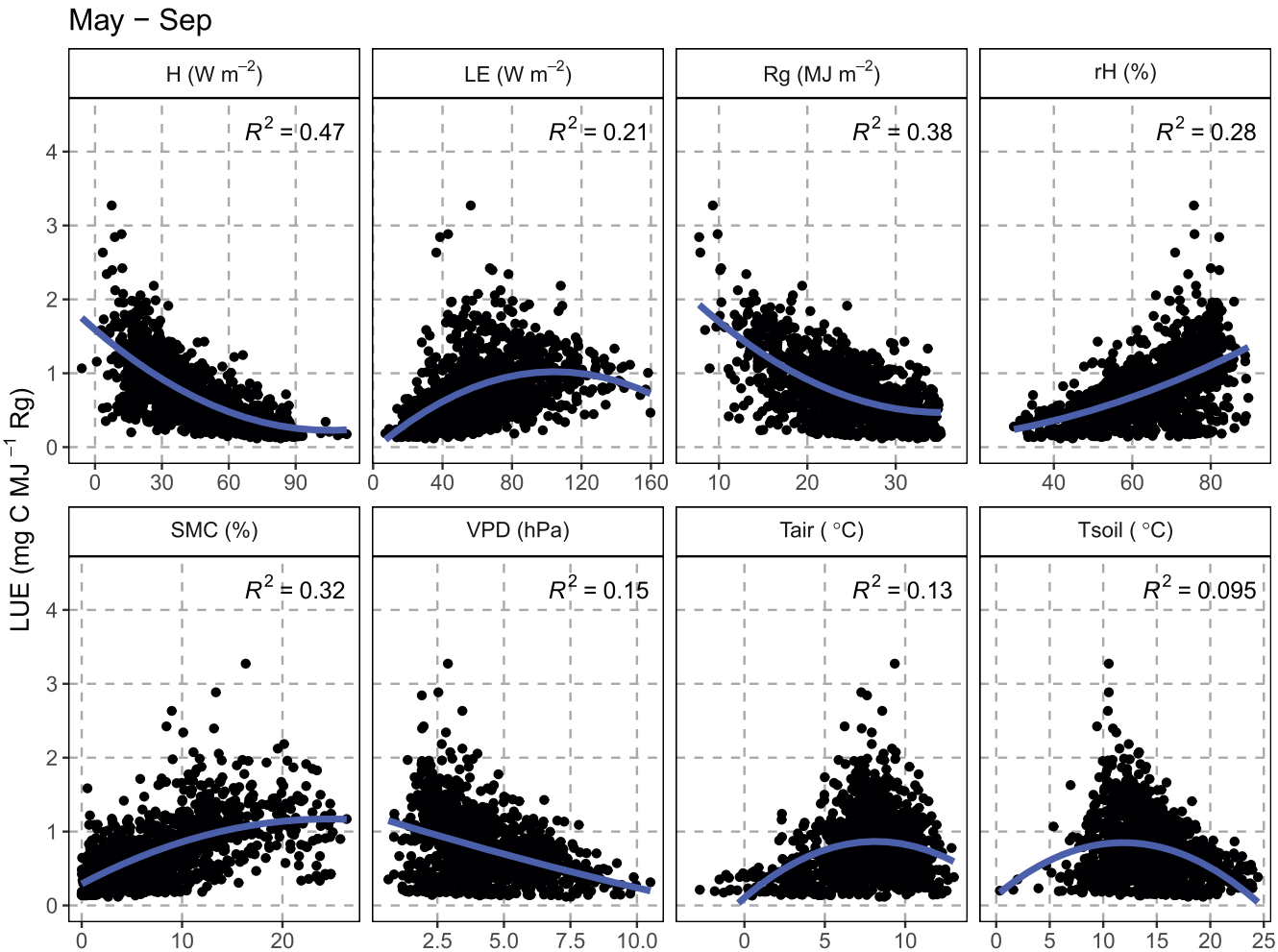

Figure 6. Relationship of daily (a) sensible heat flux (H), (b) latent heat flux (LE), (c) incoming solar radiation (Rg), (d) relative air humidity (rH), (e) soil moisture (SMC), (f) vapor pressure deficit (VPD), (g) air temperature (Tair) and (h) soil temperature (Tsoil) with LUE between May and September, using only months with >30% data availability. The blue line represents the second order polynomial regression between the variables.

greening trend is not only happening within the fenced area close to the NAMORS but all over the alpine steppe ecosystem close to the lake, as well as on the plains to the south.

We conclude that the earlier onset of summer monsoon cloud cover ameliorates drought conditions during early summer (June and July), thus increasing plant productivity and consequent carbon uptake of the alpine steppe ecosystem. On the contrary, the earlier reduction of monsoon precipitation during late summer (August and September) increases drought conditions, decreasing soil respiration more than plant productivity. Both effects lead to a net increase in ecosystem CO_2 uptake.

5. Conclusions

The TP is characterized by strong diurnal and seasonal fluctuations in radiation, heat and moisture availability. To our knowledge, this is the first study to assess the long term trends in carbon fluxes and meteorological variables alongside plant cover estimations for the Tibetan alpine steppe ecosystem. During winter (November to February) higher maximum and lower minimum temperatures cause an increased diurnal soil temperature range of more than 10°C decade^{-1}. Decreasing solar radiation during early summer (June and July) and decreasing precipitation during late summer (August and September) indicate a shift in the summer convection and precipitation dynamics toward earlier in the year. Using remotely sensed plant cover estimations, the general greening trend over the TP was also confirmed for the alpine steppe at the

south eastern shore of lake Nam Co. These changes affect the carbon cycling through different pathways: In winter, the higher maximum soil temperatures promote daytime carbon uptake while the cooling trend during night hampers soil respiration. During early summer, the changing monsoon pattern increases GPP stronger than Reco while during late summer, Reco decreases stronger than GPP. Together, these developments increase the net daily carbon uptake by roughly 0.5 g C m^{-2} $decade^{-1}$ throughout the year, thus strengthening the carbon sink strength of the Tibetan alpine steppe ecosystem at Nam Co.

Appendix A: Figures

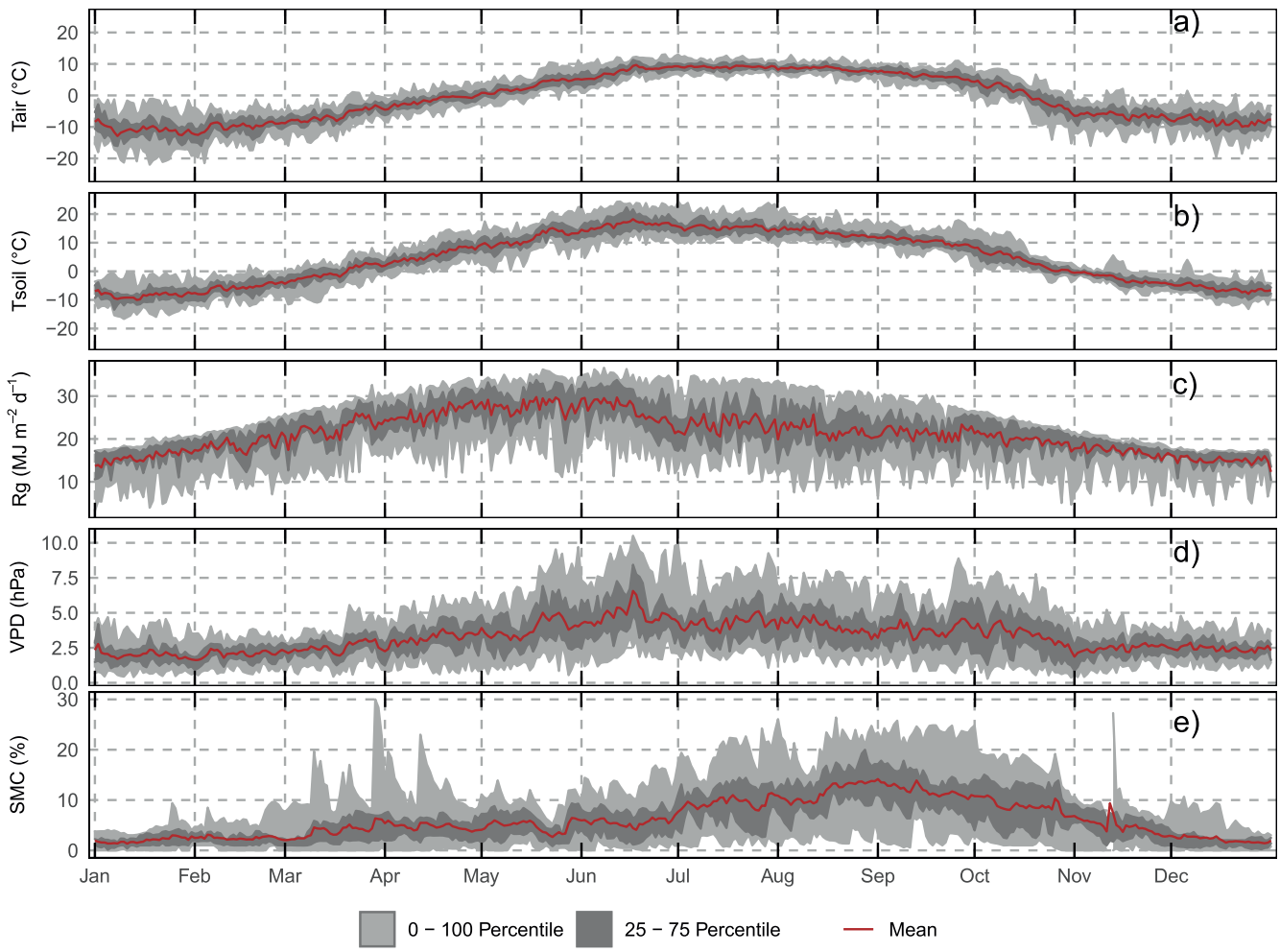

Figure A1. Mean annual course of all pooled years (2006–2019) of (a) daily air temperature (Tair), (b) soil temperature (Tsoil), (c) solar radiation (Rg), (d) vapor pressure deficit (VPD), and (e) soil moisture (SMC), as well as the 0–100 and 25–75 percentiles.

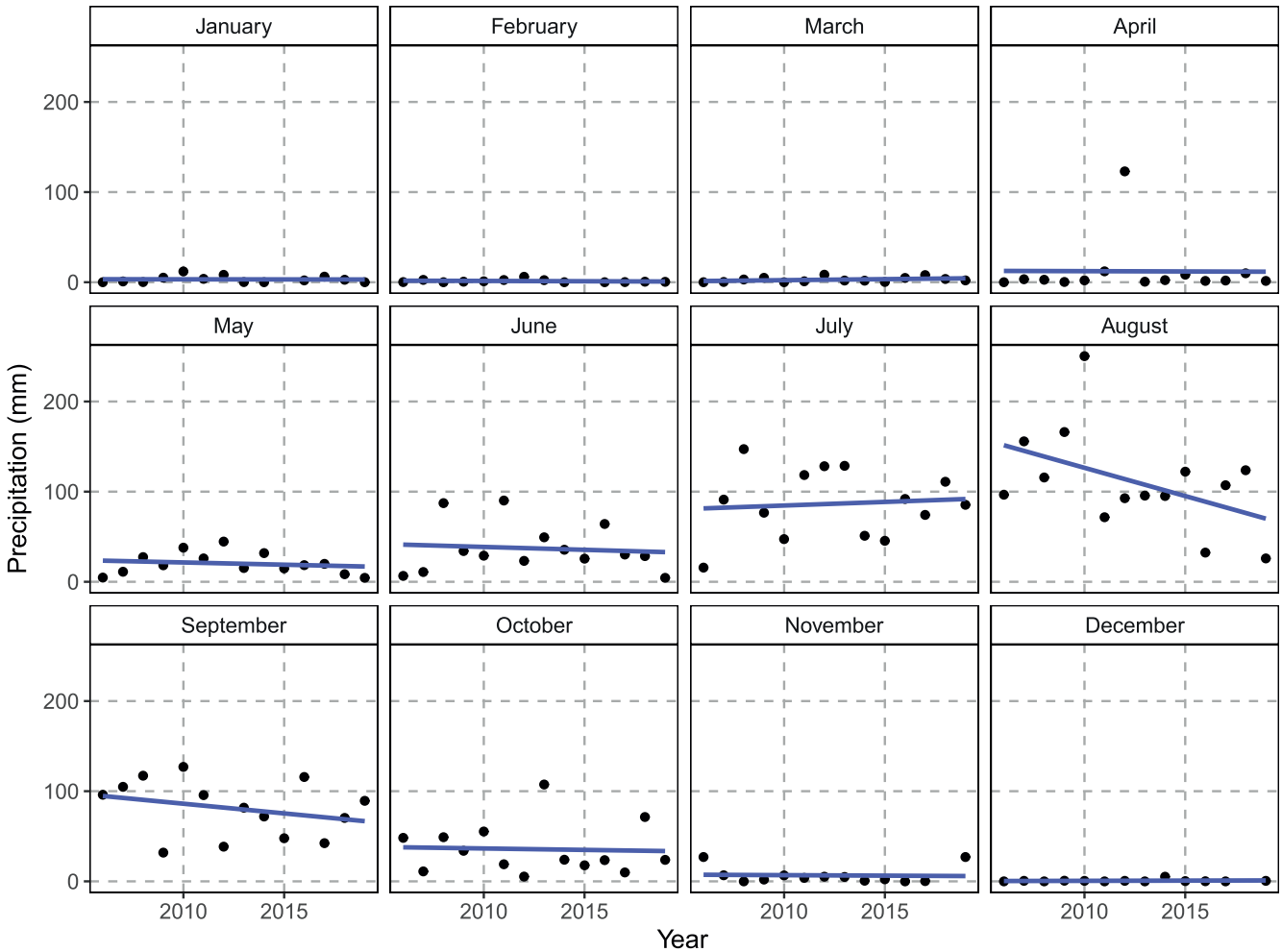

Figure A2. Monthly precipitation sums at Nam Co Station for Multi-sphere Observation and Research (NAMORS).

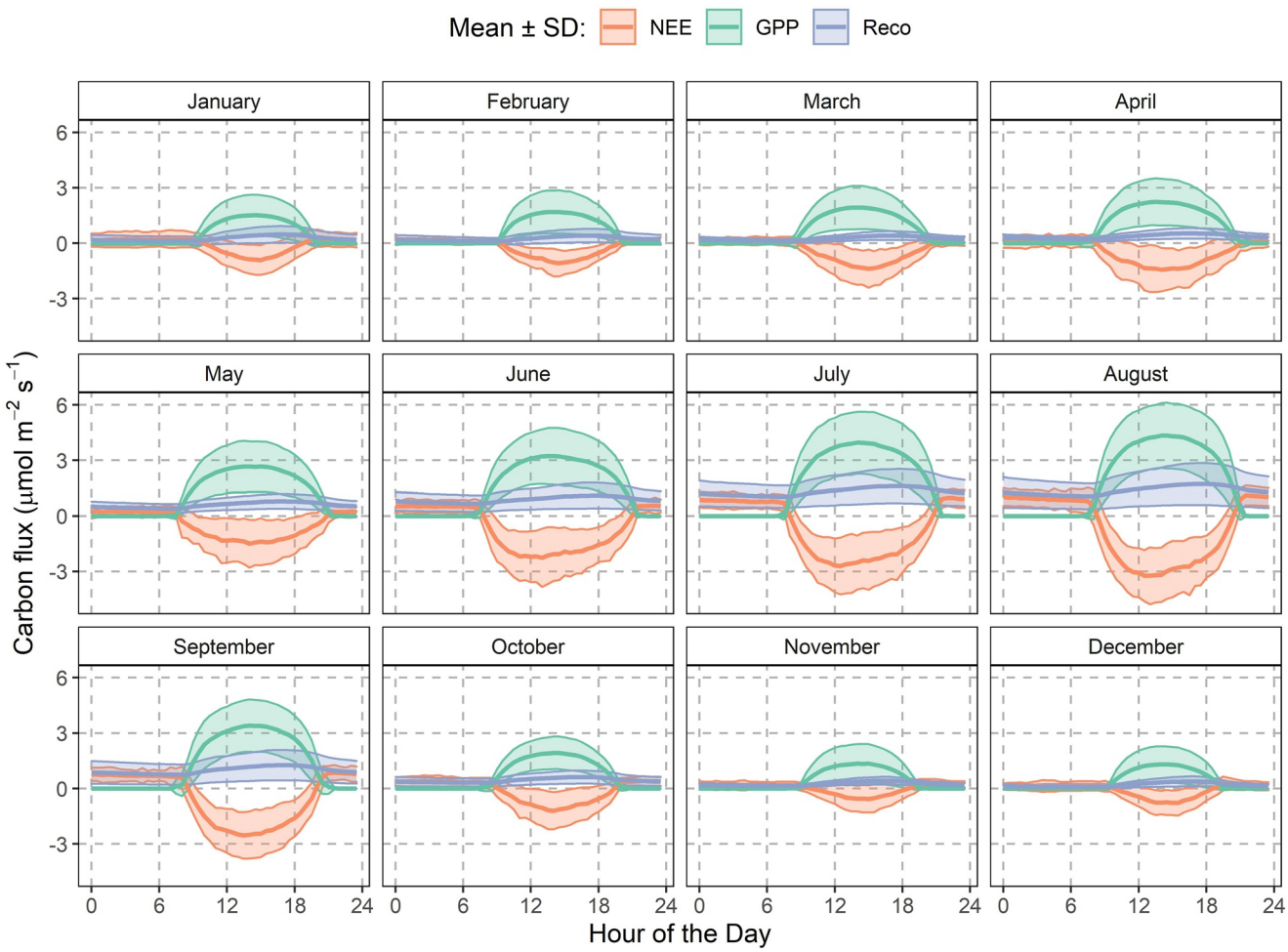

Figure A3. Mean diurnal course of carbon fluxes per Month.

Conflict Of Interest

The authors declare no conflicts of interest relevant to this study.

Data Availability Statement

The quality filtered fluxes and meteorological measurements, as well as the plant cover estimations were uploaded to the National Tibetan Plateau Data Center and can be accessed under CC BY 4.0 license via https://www.doi.org/10.11888/Meteoro.tpdc.271274 (Nieberding et al., 2021). All results, plots and tables presented in the manuscript can be reproduced using the R scripts provided in the Supporting Information S1 together with the data from the repository.

Acknowledgments
The authors like to express our gratitude to Eike Reinosch for producing the overview map (Figure 2). Furthermore, the authors would like to express our cordial thanks to Vinzenz Zerres for processing and quality checking the annual plant cover estimates. The authors warmly thank Inge Wiekenkamp for revising the original draft. This research is a contribution to the International Research Training Group "Geo-ecosystems in transition on the Tibetan Plateau (TransTiP)," funded by the Deutsche Forschungsgemeinschaft (grant no.

References

Babel, W., Biermann, T., Coners, H., Falge, E., Seeber, E., Ingrisch, J., & Foken, T. (2014). Pasture degradation modifies the water and carbon cycles of the tibetan highlands. *Biogeosciences*, *11*(23), 6633–6656. https://doi.org/10.5194/bg-11-6633-2014

Biermann, T., Babel, W., Ma, W., Chen, X., Thiem, E., Ma, Y., & Foken, T. (2014). Turbulent flux observations and modelling over a shallow lake and a wet grassland in the nam co basin, tibetan plateau. *Theoretical and Applied Climatology*, *116*(1–2), 301–316. https://doi.org/10.1007/s00704-013-0953-6

Blain, G. C. (2013). The modified mann-kendall test: On the performance of three variance correction approaches. *Bragantia*, *72*(4), 416–425. https://doi.org/10.1590/brag.2013.045

317513741/GRK 2309). It was supported by the Second Tibetan Plateau Scientific Expedition and Research (STEP) program (grant no. 2019-QZKK0103), the Strategic Priority Research Program of the Chinese Academy of Sciences (grant no. XDA20060101) and the National Natural Science Foundation of China (grant no. 91837208). The authors acknowledge support from the open-access publication funds of the Technische Universität Braunschweig. Open access funding enabled and organized by Projekt DEAL.

Chen, B., Zhang, X., Tao, J., Wu, J., Wang, J., Shi, P., & Yu, C. (2014). The impact of climate change and anthropogenic activities on alpine grassland over the qinghai-tibet plateau. *Agricultural and Forest Meteorology*, *189–190*, 11–18. https://doi.org/10.1016/j.agrformet.2014.01.002

Curatola Fernández, G., Obermeier, W., Gerique, A., López Sandoval, M., Lehnert, L., Thies, B., & Bendix, J. (2015). Land cover change in the andes of southern ecuador—patterns and drivers. *Remote Sensing*, *7*(3), 2509–2542. https://doi.org/10.3390/rs70302509

Dai, Y., Yao, T., Wang, L., Li, X., & Zhang, X. (2020). Contrasting roles of a large alpine lake on tibetan plateau in shaping regional precipitation during summer and autumn. *Frontiers of Earth Science*, *8*. https://doi.org/10.3389/feart.2020.00358

Duan, A., & Wu, G. (2006). Change of cloud amount and the climate warming on the tibetan plateau. *Geophysical Research Letters*, *33*(22), L22704. https://doi.org/10.1029/2006GL027946

Fratini, G., McDermitt, D. K., & Papale, D. (2014). Eddy-covariance flux errors due to biases in gas concentration measurements: Origins, quantification and correction. *Biogeosciences*, *11*(4), 1037–1051. https://doi.org/10.5194/bg-11-1037-2014

Friedlingstein, P., O'sullivan, M., Jones, M. W., Andrew, R. M., Hauck, J., Olsen, A., & Zaehle, S. (2020). Global carbon budget 2020. *Earth System Science Data*, *12*(4), 3269–3340. https://doi.org/10.5194/essd-12-3269-2020

Ge, F., Sielmann, F., Zhu, X., Fraedrich, K., Zhi, X., Peng, T., & Wang, L. (2017). The link between tibetan plateau monsoon and indian summer precipitation: A linear diagnostic perspective. *Climate Dynamics*, *49*(11–12), 4201–4215. https://doi.org/10.1007/s00382-017-3585-1

Gerken, T., Babel, W., Herzog, M., Fuchs, K., Sun, F., Ma, Y., & Graf, H. (2015). High-resolution modelling of interactions between soil moisture and convective development in a mountain enclosed tibetan basin. *Hydrology and Earth System Sciences*, *19*(9), 4023–4040. https://doi.org/10.5194/hess-19-4023-2015

Gerken, T., Biermann, T., Babel, W., Herzog, M., Ma, Y., Foken, T., & Graf, H. (2014). A modelling investigation into lake-breeze development and convection triggering in the nam co lake basin, tibetan plateau. *Theoretical and Applied Climatology*, *117*(1–2), 149–167. https://doi.org/10.1007/s00704-013-0987-9

Groh, J., Slawitsch, V., Herndl, M., Graf, A., Vereecken, H., & Pütz, T. (2018). Determining dew and hoar frost formation for a low mountain range and alpine grassland site by weighable lysimeter. *Journal of Hydrology*, *563*, 372–381. https://doi.org/10.1016/j.jhydrol.2018.06.009

Gu, L., Baldocchi, D., Verma, S. B., Black, T. A., Vesala, T., Falge, E. M., & Dowty, P. R. (2002). Advantages of diffuse radiation for terrestrial ecosystem productivity. *Journal of Geophysical Research*, *107*(D6), ACL 2-1–ACL 2-23. https://doi.org/10.1029/2001JD001242

Gu, S., Tang, Y., Du, M., Kato, T., Li, Y., Cui, X., & Zhao, X. (2003). Short-term variation of CO_2 flux in relation to environmental controls in an alpine meadow on the qinghai-tibetan plateau. *Journal of Geophysical Research*, *108*(D21), 4670. https://doi.org/10.1029/2003JD003584

Guo, X., Zha, T., Jia, X., Wu, B., Feng, W., Xie, J., & Peltola, H. (2016). Dynamics of dew in a cold desert-shrub ecosystem and its abiotic controls. *Atmosphere*, *7*(3), 32. https://doi.org/10.3390/atmos7030032

Hamed, K. H., & Rao, A. R. (1998). A modified mann-kendall trend test for autocorrelated data. *Journal of Hydrology*, *204*(1–4), 182–196. https://doi.org/10.1016/S0022-1694(97)00125-X

Huang, K., Wang, S., Zhou, L., Wang, H., Zhang, J., Yan, J., & Shi, P. (2014). Impacts of diffuse radiation on light use efficiency across terrestrial ecosystems based on eddy covariance observation in china. *PloS One*, *9*(11), e110988. https://doi.org/10.1371/journal.pone.0110988

Jarvis, A., Reuter, H., Nelson, A., & Guevara, E. (2008). Hole-filled seamless srtm data v4. International Centre for Tropical Agriculture (CIAT).

Joos, F., & Spahni, R. (2008). Rates of change in natural and anthropogenic radiative forcing over the past 20,000 years. *Proceedings of the National Academy of Sciences of the United States of America*, *105*(5), 1425–1430. https://doi.org/10.1073/pnas.0707386105

Kato, T., Tang, Y., Gu, S., Hirota, M., Du, M., Li, Y., & Zhao, X. (2006). Temperature and biomass influences on interannual changes in co2 exchange in an alpine meadow on the qinghai-tibetan plateau. *Global Change Biology*, *12*(7), 1285–1298. https://doi.org/10.1111/j.1365-2486.2006.01153.x

Kato, T., Tang, Y., Song, G., Hirota, M., Cui, X., Du, M., & Oikawa, T. (2004). Seasonal patterns of gross primary production and ecosystem respiration in an alpine meadow ecosystem on the qinghai-tibetan plateau. *Journal of Geophysical Research*, *109*(D12), 711. https://doi.org/10.1029/2003JD003951

Körner, C. (1995). Leaf diffusive conductances in the major vegetation types of the globe. In E.-D. Schulze, & M. M. Caldwell (Eds.), *Ecophysiology of photosynthesis* (pp. 463–490). Berlin: Springer. https://doi.org/10.1007/978-3-642-79354-7_22

Lasslop, G., Reichstein, M., Papale, D., Richardson, A. D., Arneth, A., Barr, A., & Wohlfahrt, G. (2010). Separation of net ecosystem exchange into assimilation and respiration using a light response curve approach: Critical issues and global evaluation. *Global Change Biology*, *16*(1), 187–208. https://doi.org/10.1111/j.1365-2486.2009.02041.x

Lehnert, L. W., Meyer, H., Wang, Y., Miehe, G., Thies, B., Reudenbach, C., & Bendix, J. (2015). Retrieval of grassland plant coverage on the tibetan plateau based on a multi-scale, multi-sensor and multi-method approach. *Remote Sensing of Environment*, *164*, 197–207. https://doi.org/10.1016/j.rse.2015.04.020

Li, Q. (2018). Spatial variability and long-term change in pollen diversity in nam co catchment (central tibetan plateau): Implications for alpine vegetation restoration from a paleoecological perspective. *Science China Earth Sciences*, *61*(3), 270–284. https://doi.org/10.1007/s11430-017-9133-0

Li, X., Guo, W., Chen, J., Ni, X., & Wei, X. (2019). Responses of vegetation green-up date to temperature variation in alpine grassland on the tibetan plateau. *Ecological Indicators*, *104*, 390–397. https://doi.org/10.1016/j.ecolind.2019.05.003

Liu, Y., Chen, H., Zhang, G., Sun, J., & Wang, H. (2019). The advanced south asian monsoon onset accelerates lake expansion over the tibetan plateau. *Science Bulletin*, *64*(20), 1486–1489. https://doi.org/10.1016/j.scib.2019.08.011

Liu, Y., Tenzintarchen, Geng, X., Wei, D., Dai, D., & Xu, -R. (2020). Grazing exclusion enhanced net ecosystem carbon uptake but decreased plant nutrient content in an alpine steppe. *Catena*, *195*, 104799. https://doi.org/10.1016/j.catena.2020.104799

Ma, N., Szilagyi, J., Niu, G.-Y., Zhang, Y., Zhang, T., Wang, B., & Wu, Y. (2016). Evaporation variability of nam co lake in the tibetan plateau and its role in recent rapid lake expansion. *Journal of Hydrology*, *537*, 27–35. https://doi.org/10.1016/j.jhydrol.2016.03.030

Ma, Y., Ma, W., Zhong, L., Hu, Z., Li, M., Zhu, Z., & Liu, X. (2017). Monitoring and modeling the tibetan plateau's climate system and its impact on east asia. *Scientific Reports*, *7*, 44574. https://doi.org/10.1038/srep44574

Ma, Y., Wang, Y., Wu, R., Hu, Z., Yang, K., Li, M., & Ishikawa, H. (2009). Recent advances on the study of atmosphere-land interaction observations on the tibetan plateau. *Hydrology and Earth System Sciences*, *13*(7), 1103–1111. https://doi.org/10.5194/hess-13-1103-2009

Miehe, G., Bach, K., Miehe, S., Kluge, J., Yongping, Y., Duo, L., Wesche, K. (2011). Alpine steppe plant communities of the tibetan highlands. *Applied Vegetation Science*, *14*(4), 547–560. https://doi.org/10.1111/j.1654-109X.2011.01147.x

Miehe, G., Schleuss, P.-M., Seeber, E., Babel, W., Biermann, T., Braendle, M., & Wesche, K. (2019). The kobresia pygmaea ecosystem of the tibetan highlands — Origin, functioning and degradation of the world's largest pastoral alpine ecosystem: Kobresia pastures of tibet. *The Science of the Total Environment*, *648*, 754–771. https://doi.org/10.1016/j.scitotenv.2018.08.164

Nieberding, F., Ma, Y., Ma, W., Wang, Y., Sachs, T., Lehnert, L., et al. (2021). Half-hourly eddy covariance fluxes, gap-filled meteorological variables, precipitation and remotely sensed plant cover estimations from namors between 2005 and 2020: Data set. *National Tibetan Plateau Data Center*. https://doi.org/10.11888/Meteoro.tpdc.271274

Nieberding, F., Wille, C., Fratini, G., Asmussen, M. O., Wang, Y., Ma, Y., & Sachs, T. (2020). A long term (2005–2019) eddy covariance data set of CO_2 and H_2O fluxes from the tibetan alpine steppe. *Earth System Science Data*. https://doi.org/10.5194/essd-2020-63

NOAA National Centers for Environmental Information. (2021). *State of the climate: Global climate report for annual 2020*. Retrieved from https://www.ncdc.noaa.gov/sotc/global/202013

Patakamuri, S. K., & O'Brien, N. (2020). *Modifiedmk: Modified versions of mann kendall and spearman's rho trend tests: R package version 1.5.0*.

Pei, Z.-Y., Ouyang, H., Zhou, C.-P., & Xu, X.-L. (2009). Carbon balance in an alpine steppe in the qinghai-tibet plateau. *Journal of Integrative Plant Biology*, *51*(5), 521–526. https://doi.org/10.1111/j.1744-7909.2009.00813.x

Qiu, J. (2008). China: The third pole. *Nature*, *454*(7203), 393–396. https://doi.org/10.1038/454393a

Reis, M. G. d., & Ribeiro, A. (2020). Conversion factors and general equations applied in agricultural and forest meteorology. *Agrometeoros*, *27*(2), 227–258. https://doi.org/10.31062/agrom.v27i2.26527

Riano, D., Chuvieco, E., Salas, J., & Aguado, I. (2003). Assessment of different topographic corrections in landsat-tm data for mapping vegetation types (2003). *IEEE Transactions on Geoscience and Remote Sensing*, *41*(5), 1056–1061. https://doi.org/10.1109/TGRS.2003.811693

Sen, P. K. (1968). Estimates of the regression coefficient based on kendall's tau. *Journal of the American Statistical Association*, *63*(324), 1379. https://doi.org/10.2307/2285891

Shen, M., Piao, S., Chen, X., An, S., Fu, Y. H., Wang, S., & Janssens, I. A. (2016). Strong impacts of daily minimum temperature on the green-up date and summer greenness of the tibetan plateau. *Global Change Biology*, *22*(9), 3057–3066. https://doi.org/10.1111/gcb.13301

Shen, M., Tang, Y., Chen, J., Zhu, X., & Zheng, Y. (2011). Influences of temperature and precipitation before the growing season on spring phenology in grasslands of the central and eastern qinghai-tibetan plateau. *Agricultural and Forest Meteorology*, *151*(12), 1711–1722. https://doi.org/10.1016/j.agrformet.2011.07.003

Vermote, E. F., Tanre, D., Deuze, J. L., Herman, M., & Morcette, J.-J. (1997). Second simulation of the satellite signal in the solar spectrum, 6s: An overview. *IEEE Transactions on Geoscience and Remote Sensing*, *35*(3), 675–686. https://doi.org/10.1109/36.581987

Wang, F., Shao, W., Yu, H., Kan, G., He, X., Zhang, D., & Wang, G. (2020). Re-evaluation of the power of the mann-kendall test for detecting monotonic trends in hydrometeorological time series. *Frontiers of Earth Science*, *8*. https://doi.org/10.3389/feart.2020.00014

Wang, H., Liu, H., Cao, G., Ma, Z., Li, Y., Zhang, F., & He, J.-S. (2020). Alpine grassland plants grow earlier and faster but biomass remains unchanged over 35 years of climate change. *Ecology Letters*, *23*, 701–710. https://doi.org/10.1111/ele.13474

Wang, L., Liu, H., Shao, Y., Liu, Y., & Sun, J. (2016). Water and CO_2 fluxes over semiarid alpine steppe and humid alpine meadow ecosystems on the tibetan plateau. *Theoretical and Applied Climatology*, *131*(1–2), 547–556. https://doi.org/10.1007/s00704-016-1997-1

Wang, X., Pang, G., & Yang, M. (2018). Precipitation over the tibetan plateau during recent decades: A review based on observations and simulations. *International Journal of Climatology*, *38*(3), 1116–1131. https://doi.org/10.1002/joc.5246

Wang, Y., Zhu, Z., Ma, Y., & Yuan, L. (2020). Carbon and water fluxes in an alpine steppe ecosystem in the nam co area of the tibetan plateau during two years with contrasting amounts of precipitation. *International journal of biometeorology*. https://doi.org/10.1007/s00484-020-01892-2

Wasserstein, R. L., & Lazar, N. A. (2016). The asa statement on p -values: Context, process, and purpose. *The American Statistician*, *70*(2), 129–133. https://doi.org/10.1080/00031305.2016.1154108

Wasserstein, R. L., Schirm, A. L., & Lazar, N. A. (2019). Moving to a world beyond "p < 0.05". *The American Statistician*, *73*, 1–19. https://doi.org/10.1080/00031305.2019.1583913

Wei, D., Ri, X., Liu, Y., Wang, Y., & Wang, Y. (2014). Three-year study of CO_2 efflux and CH_4/N_2O fluxes at an alpine steppe site on the central tibetan plateau and their responses to simulated n deposition. *Geoderma*, *232–234*, 88–96. https://doi.org/10.1016/j.geoderma.2014.05.002

Wei, D., Ri, X., Wang, Y., Wang, Y., Liu, Y., & Yao, T. (2012). Responses of CO_2, CH_4 and N_2O fluxes to livestock exclosure in an alpine steppe on the tibetan plateau, china. *Plant and Soil*, *359*(1–2), 45–55. https://doi.org/10.1007/s11104-011-1105-3

Wei, Y., Wang, S., Fang, Y., & Nawaz, Z. (2017). Integrated assessment on the vulnerability of animal husbandry to snow disasters under climate change in the qinghai-tibetan plateau. *Global and Planetary Change*, *157*, 139–152. https://doi.org/10.1016/j.gloplacha.2017.08.017

Wutzler, T., Lucas-Moffat, A., Migliavacca, M., Knauer, J., Sickel, K., Šigut, L., & Reichstein, M. (2018). Basic and extensible post-processing of eddy covariance flux data with reddyproc. *Biogeosciences*, *15*(16), 5015–5030. https://doi.org/10.5194/bg-15-5015-2018

Yang, K., Wu, H., Qin, J., Lin, C., Tang, W., & Chen, Y. (2014). Recent climate changes over the tibetan plateau and their impacts on energy and water cycle: A review. *Global and Planetary Change*, *112*, 79–91. https://doi.org/10.1016/j.gloplacha.2013.12.001

Yang, K., Ye, B., Zhou, D., Wu, B., Foken, T., Qin, J., & Zhou, Z. (2011). Response of hydrological cycle to recent climate changes in the tibetan plateau. *Climatic Change*, *109*(3–4), 517–534. https://doi.org/10.1007/s10584-011-0099-4

Yang, Y., Dong, C., Yang, S., Li, X., Sun, X., & Yang, Y. (2015). Physiological and proteomic adaptation of the alpine grass stipa purpurea to a drought gradient. *PloS One*, *10*(2), e0117475. https://doi.org/10.1371/journal.pone.0117475

Yang, Y., & Ren, R. (2017). On the contrasting decadal changes of diurnal surface temperature range between the tibetan plateau and southeastern china during the 1980s–2000s. *Advances in Atmospheric Sciences*, *34*(2), 181–198. https://doi.org/10.1007/s00376-016-6077-z

Yao, T., Masson-Delmotte, V., Gao, J., Yu, W., Yang, X., Risi, C., & Hou, S. (2013). A review of climatic controls on $\delta^{18}o$ in precipitation over the tibetan plateau: Observations and simulations. *Reviews of Geophysics*, *51*(4), 525–548. https://doi.org/10.1002/rog.20023

Yao, T., Xue, Y., Chen, D., Chen, F., Thompson, L., Cui, P., & Li, Q. (2019). Recent third pole's rapid warming accompanies cryospheric melt and water cycle intensification and interactions between monsoon and environment: Multidisciplinary approach with observations, modeling, and analysis. *Bulletin of the American Meteorological Society*, *100*(3), 423–444. https://doi.org/10.1175/BAMS-D-17-0057.1

You, G., Arain, M. A., Wang, S., McKenzie, S., Zou, C., Wang, Z., & Gao, J. (2019). The spatial-temporal distributions of controlling factors on vegetation growth in tibet autonomous region, southwestern china. *Environmental Research Communications*, *1*(9), 091003. https://doi.org/10.1088/2515-7620/ab3d87

You, Q., Min, J., Jiao, Y., Sillanpää, M., & Kang, S. (2016). Observed trend of diurnal temperature range in the tibetan plateau in recent decades. *International Journal of Climatology*, *36*(6), 2633–2643. https://doi.org/10.1002/joc.4517

Yue, S., Pilon, P., Phinney, B., & Cavadias, G. (2002). The influence of autocorrelation on the ability to detect trend in hydrological series. *Hydrological Processes*, *16*(9), 1807–1829. https://doi.org/10.1002/hyp.1095

Yue, S., & Wang, C. (2004). The mann-kendall test modified by effective sample size to detect trend in serially correlated hydrological series: Water resources management. *Water Resources Management*, *18*(3), 201–218. https://doi.org/10.1023/B:WARM.0000043140.61082.60

Yue, S., & Wang, C. Y. (2002). Applicability of prewhitening to eliminate the influence of serial correlation on the mann-kendall test. *Water Resources Research*, *38*(6), 4-1–4-7. https://doi.org/10.1029/2001WR000861

Zhang, G., Zhang, Y., Dong, J., & Xiao, X. (2013). Green-up dates in the tibetan plateau have continuously advanced from 1982 to 2011. *Proceedings of the National Academy of Sciences of the United States of America*, *110*(11), 4309–4314. https://doi.org/10.1073/pnas.1210423110

Zhang, T., Zhang, Y., Xu, M., Zhu, J., Chen, N., Jiang, Y., & Yu, G. (2018). Water availability is more important than temperature in driving the carbon fluxes of an alpine meadow on the tibetan plateau. *Agricultural and Forest Meteorology*, *256–257*, 22–31. https://doi.org/10.1016/j.agrformet.2018.02.027

Zhang, W., Zhou, T., & Zhang, L. (2017). Wetting and greening tibetan plateau in early summer in recent decades. *Journal of Geophysical Research: Atmospheres*, *122*(11), 5808–5822. https://doi.org/10.1002/2017JD026468

Zhao, J., Li, R., Li, X., & Tian, L. (2017). Environmental controls on soil respiration in alpine meadow along a large altitudinal gradient on the central tibetan plateau. *Catena*, *159*, 84–92. https://doi.org/10.1016/j.catena.2017.08.007

Zhao, J., Luo, T., Li, R., Wei, H., Li, X., Du, M., & Tang, Y. (2018). Precipitation alters temperature effects on ecosystem respiration in tibetan alpine meadows. *Agricultural and Forest Meteorology*, *252*, 121–129. https://doi.org/10.1016/j.agrformet.2018.01.014

Zheng, Z., Zhu, W., Chen, G., Jiang, N., Fan, D., & Zhang, D. (2016). Continuous but diverse advancement of spring-summer phenology in response to climate warming across the qinghai-tibetan plateau. *Agricultural and Forest Meteorology*, *223*, 194–202. https://doi.org/10.1016/j.agrformet.2016.04.012

Zhou, Y., Webster, R., Viscarra Rossel, R. A., Shi, Z., & Chen, S. (2019). Baseline map of soil organic carbon in tibet and its uncertainty in the 1980s. *Geoderma*, *334*, 124–133. https://doi.org/10.1016/j.geoderma.2018.07.037

Zhu, Z., Ma, Y., Li, M., Hu, Z., Xu, C., Zhang, L., & Ichiro, T. (2015). Carbon dioxide exchange between an alpine steppe ecosystem and the atmosphere on the nam co area of the tibetan plateau. *Agricultural and Forest Meteorology*, *203*, 169–179. https://doi.org/10.1016/j.agrformet.2014.12.013